Metamodel applied to fatigue damage in overhead lines conductors

Julien SAID[1]*, Sami EL IDRISSI RAGHNI[2], Maxime GUEGUIN[2], Emmanuel CIEREN[2], Laura COHEN[1], Fikri HAFID[1], Jean-Michel GHIDAGLIA[3], Marc COULANGEON[4], Jérome BROCARD[4]
1 – RTE R&D, Immeuble Window, 7 place du dôme, 92073 La Défense, FRANCE
2 – Eurobios, 61 avenue du Président Wilson, 94230 Cachan, FRANCE
3 – Centre Borelli, ENS Paris-Saclay, CNRS, Univ. Paris-Saclay, 91190 Gif-sur-Yvette,
4 – Dervaux, SICAME GROUP, 42500 Le Chambon-Feugerolles, France

julien.said@rte-france.com; sami.elidrissi@eurobios.com; mgueguin@eurobios.com; ecieren@eurobios.com; laura.cohen@rte-france.com; fikri.hafid@rte-france.com; ghidaglia@free.fr; mcoulangeon@dervaux.fr; jbrocard@dervaux.fr

SUMMARY

Mechanical fatigue in overhead line conductors is one of the major concerns for Transmission Systems Operators (TSO). This phenomenon occurs due to cyclic vibration of the cable, mainly caused by wind loadings. These vibrations are likely to nucleate and propagate cracks that could ultimately lead to strand failures. Hence, a reliable prediction of conductor' lifetime could help adapting the maintenance or repair protocols for the entire grid.

In order to better assess this risk, experimental data have been produced over the past few decades, giving access to a wide range of fatigue curves depending on the conductor type and the vibration amplitude. The fatigue endurance is then defined by the number of cycles before failure of a given number of constituent strands, usually three. Thanks to the standardisation work of Cigre members, the results produced from experimental campaigns can be compared to one another, and also to the well-known Safe Border Line. Moreover, additional parameters could be considered to extend the applicability of this safe limit. For instance, it does not account for the conductor angle outside the clamping zone or AAAC. Thus, the main goal of this contribution is to propose a simple predictive model of the behaviour of vibrating conductors. It relies on a hybrid approach that considers experimental results and statistical data analysis. This tool could be used to complete the Safe Border Line and extend our knowledge on how overhead lines age and decay.

To achieve that, a database is first presented that contains more than two hundred tests described in the literature. This database includes several configurations of tests performed on overhead lines conductors, either ASCR or AAAC. Then, a machine learning data-driven model is proposed to predict the endurance of a conductor using a few analytical explanatory variables such as the conductor's stiffness or its geometrical orientation. These variables are based on a state-of-the-art formula that can be computed directly from the mechanical loadings or the conductor's geometry.

KEYWORDS

Overhead conductors, mechanical fatigue, machine learning algorithm, predictive model, safe design zone

1 INTRODUCTION

The lifetime assessment of overhead conductors has become a key point for any Transmission System Operator (TSO) in charge of an electrical power grid. In order to adapt their future maintenance and repair policies, they need to be able to predict the mechanical behaviour of their power lines with physical understanding and accuracy.

The ageing of these conductors is caused by many phenomena, including corrosion, mechanical fatigue, fretting-fatigue occurring between stranded wires, etc. In this work, mechanical fatigue is specifically addressed and a predictive workflow is developed in order to propose a consistent safe limit. This damaging mechanism is related to the wind-induced oscillations, from which the most common phenomena are the so-called Aeolian vibrations. This problem has been known for several decades, and various methods have been investigated in the literature to get a comprehensive understanding on how conductors age and may ultimately fail. One of the most common approaches consists in using technological test benches where an entire portion of conductor is put in motion to witness its behaviour [1] – [5]. It can be used to assess self-damping properties, line equipment and of course the fatigue endurance for a given set of loading conditions. The associated outcomes are extremely valuable and useful for further design and modelling efforts, but require very specific and expensive facilities to be able to run such tests. Still, more and more data are available and described in the literature as this topic keeps gaining interest over the years.

To capitalize on this growing source of data, the work described in this paper proposes a first statistical approach with a simple machine learning algorithm trained on these conductor tests. The linear quantile regression is used to predict the fatigue lifetime to failure of various types of conductors, and is meant to be compared with the commonly used Safe Border Line defined by CIGRE (defined in [10]).

2 CONDUCTOR FATIGUE AND ENDURANCE LIMITS

Determining and proposing a safe method to ensure the sustainability of powerline design according to their location and expected loading has been a key issue for TSOs and associated institutes or communities. As summed up in [6], IEEE, EPRI and CIGRE all proposed tools to estimate the failure risk according to key parameters such as the vibrating amplitude or the estimated stress.

2.1. Endurance limit approach

This kind of approach has been proposed by both IEEE and EPRI and assumes that as long as the vibration levels remain below a given limit, the conductor will display an infinite life. The safe values for stress are determined so as to prevent suchs limits from being exceeded. For instance, the IEEE Transmission and Distribution Committee recommends to directly measure the vibrating amplitude at a distance $Xb = 89$ mm (3.5 inches) from the clamp. The associated deflection corresponds to Yb, and can be compared to safe values available in the literature. The EPRI proposed a similar strategy, in which the safe limit is based on the maximum dynamic stress. This stress is related to the bending amplitude Yb through the so-called

Poffenberger-Swart formula [7] and allows to account for the bending stiffness or the conductor diameter.

$$\sigma_a = K.Yb \qquad (1)$$

With:

$$K = \frac{E.d.p^2}{4(e^{-p.Xb}-1+p.Xb)} \qquad (2)$$

$$p = \sqrt{\frac{H}{(EI)_{min}}} \qquad (3)$$

In the previous equations, σ_a is the maximum bending stress, H the mechanical tension of the conductor, E the Young's modulus of outer layers, d the diameter of the outer layer strands and finally EI_{min} the minimum bending stiffness. This particular stiffness correspond to the limit case where all strands are considered independant.

However, the current work rather focuses on the approach described in the following section.

2.2. Cumulative damage approach

The recommandation of the CIGRE International Council relies on a cumulative damage approach based on various "Cycles to failure" curves, also called S-N or Wöhler curves. Some of these curves are plotted on figure 1, with the associated data being obtained for several types of conductors and materials, coming for various laboratories and available in reference [8]. The Safe Border Line has then been established according to the Miner's law of cumulative damage [9], and the resulting curve is compared to other S-N curves illustrated in figure 1.
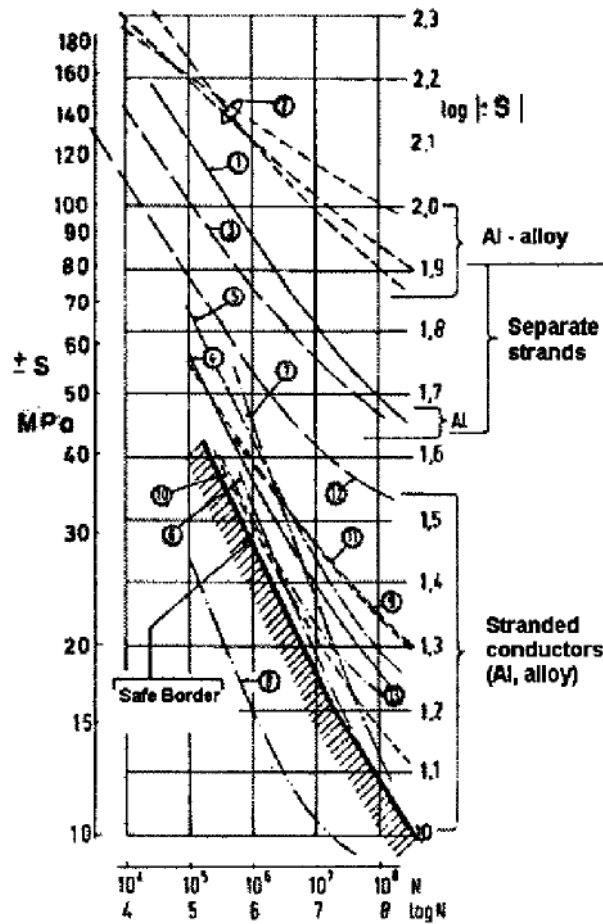
Figure 1: plots of S-N curves for overhead conductors compiled by CIGRE and the Safe Border Line

This safe border is meant to be conservative and gives an estimate of the lifetime to failure associated with a given stress suffered by the conductor. The usual recommendations for TSOs suggest to use this SBL when fatigue curves for the exact same type of conductor to use are not available.

2.3. Construction of a conductor's fatigue comprehensive dataset

One of the first steps of the proposed method consisted in a literature review in order to gather actual fatigue data for various types of conductors. As many authors from distinct countries shared their valuable results thanks to their published work, being able to gather such figures may offer a great basis for anyone working in the field of conductor vibrations to start with. These data are summed up and displayed in the appendix. As it can be seen in this table accounting for more than 200 tests, many types of conductor are listed and can be divided into two main families. These two families are ACSR (Aluminium Conductor Steel Reinforced) conductors, and AAAC (All Aluminium Alloy) conductors. All entries were also anonymized as it is commonly done in the field of data science.

Finally, in addition to these data obtained thanks to the literature, new tests are being conducted in a dedicated facilities on ACSR and AAAC conductors (figure 2). These new results are to be confronted on future predictive results and reinforce this data-driven statistical strategy.

4
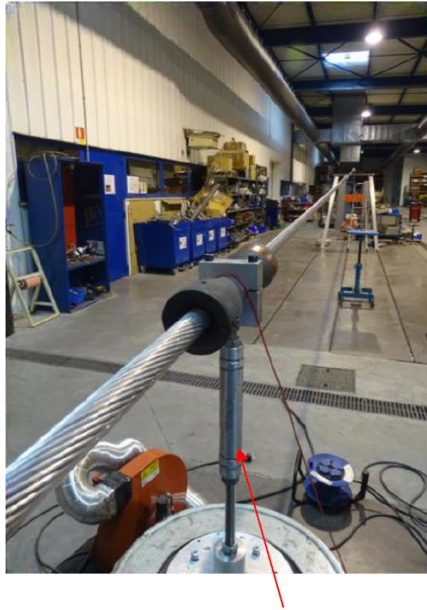
Vibrating actuator

Figure 2: experimental test bench with an ACSR conductor linked to a vibrating actuator

3 STATISTICAL REGRESSION MODEL

The purpose of this section is to briefly introduce the quantile regression algorithm and how it has been applied on the conductor's fatigue dataset.

3.1. Definition of the quantile regression

The quantile regression is similar to the well-known linear but aims at different statistical values. Whereas the least square method used for linear regression estimates the mean value of the response variable, the quantile regression estimates the median or any other quantile of the response variable.

Figure 3 illustrates this method for an arbitrary set of (x ; y) data. It compares three quantile regressions and the regular linear regression. First, it shows that even though the quantile regression at 50% (*i.e.* the median) and the linear one are very close, they are not superimposed, just like the mean and median. Furthermore, the other regressions give a reliable bounded domain containing 95% of the total data set. It can be very useful to assess inferior or superior bounds according to the application.
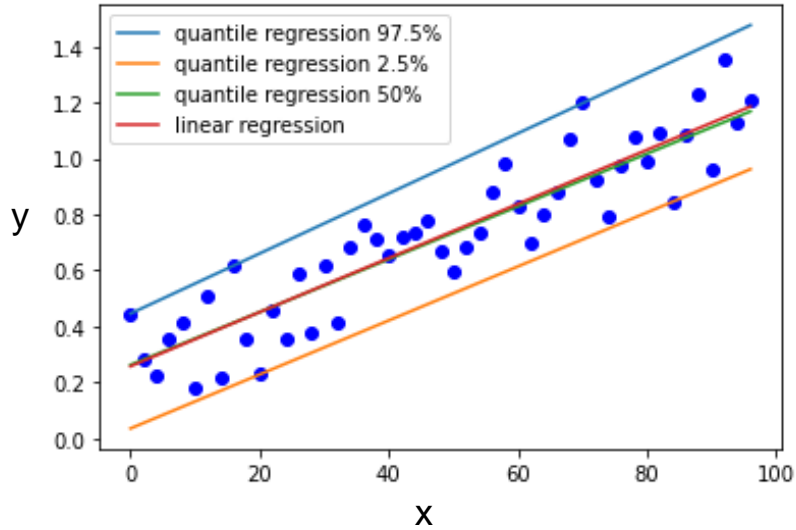
Figure 3: comparison of 3 quantile regressions and the linear regression (according to the least square method) on an arbitrary set of data

In the next sections, it will be shown that aiming at the 2.5% quantile can offer an interesting safe limit for fatigue predictions and design. This type of regression is also known for its good ability to be extrapolated with a limited risk of over-fitting.

3.2. Quantile regression on conductor's fatigue data

Machine learning algorithms consider two main objects: a target vector and a feature vector. On the one hand, the target represents what the algorithm will try to predict. In figure 2, the target is the scalar y, and in conductor's fatigue, the target is typically the lifetime to failure. On the other hand, the features are the input parameters contained in the initial dataset. Hence, in figure 2, there is only one feature and it is the scalar x. When the regression model is set up, for one feature vector (containing one or more features), there is one prediction.

For the current case of study, four features X_i are used to characterize the conductor's lifespan, depending on the boundary conditions and the conductor itself. These four features are:

- The normalized mechanical tension

$$X_1 = \frac{H}{RTS} \tag{4}$$

With H the mechanical tension and RTS the Rated Tensile Strength (i.e. the maximum tensile load that can be applied on the corresponding conductor).

- The normalized vibration amplitude

$$X_2 = \log\left(\frac{Yb}{D}\right) \tag{5}$$

With Yb the vibration amplitude introduced in section 2.1 and D the conductor's nominal diameter.

- The normalized *self-weight* (sw) induced displacement

$$X_3 = \frac{U_{sw}}{D} \qquad (6)$$

Such as:

$$\sigma_{sw} = K_{norm} . \frac{U_{sw}}{D} . E \qquad (7)$$

With σ_{sw} the self-weight induced stress, E the Young's Modulus of the outer layer and K_{norm} a normalized parameter described below. U_{sw} corresponds to the displacement solely caused by the self-weight of the conductor itself. It can thus be noted that U_{sw} can be calculated through the catenary equation. Hence, for experimental tests, it is manually imposed by acting on the conductor's angle outside of the clamping zone.

- The normalized stress coefficient K_{norm}.

$$X_4 = K_{norm} \qquad (8)$$

It comes from the Pofferberger-Swart formalism, by applying equation (1) (section 2.1) and replacing Yb by U_{sw} (as it is done for σ_{sw} in the equation above). Thus, it depends on the conductor's geometry and materials.

These features may also be referred as explanatory variables, as they are the most likely to affect the final response of the system. More variables could be taken into consideration, but these four are believed to have the most significant influence of the lifetime to failure for a given conductors.

Knowing these four features, any linear regression will be expressed as follows:

$$\log(N) = a_0 + a_1 . X_1 + a_2 . X_2 + a_3 . X_3 + a_4 . X_4 \qquad (9)$$

Where N represents the predicted lifetime to failure and a_i the coefficients defining a given model. These values depend on the regression used. For both 2.5% and 97.5% quantile regressions, the associated a_i are listed in table 1.

Table 1 : lists of coefficients used to define the two quantile regression models described in this study

	a_0	a_1	a_2	a_3	a_4
2.5% quantile regression	6.15	1.37	-2.06	-2.45	-165
97.5% quantile regression	6.01	-4.58	-2.20	-1.08	-43.5

Thanks to these values, an interested reader working in the field of conductor's fatigue may use it to try to predict future tests to conduct or compare it with its own data. Any feedback to the authors of this study would also be greatly appreciated.

4 COMPARISONS WITH THE SBL

4.1. SBL versus literature fatigue data

Before applying any statistical regression, it can be insightful to compare the Safe Border Line to the plot of all the results listed in the first appendix. This comparison is shown in figure 4, where all data are plotted in the S-N plane versus the Safe Border Line. On this plot, non-censored points mean that the corresponding tests displayed wire failures, while censored ones were stopped before witnessing any breakage. The visible scatter comes from the fact that this plot gather several types of conductor with various loading conditions.
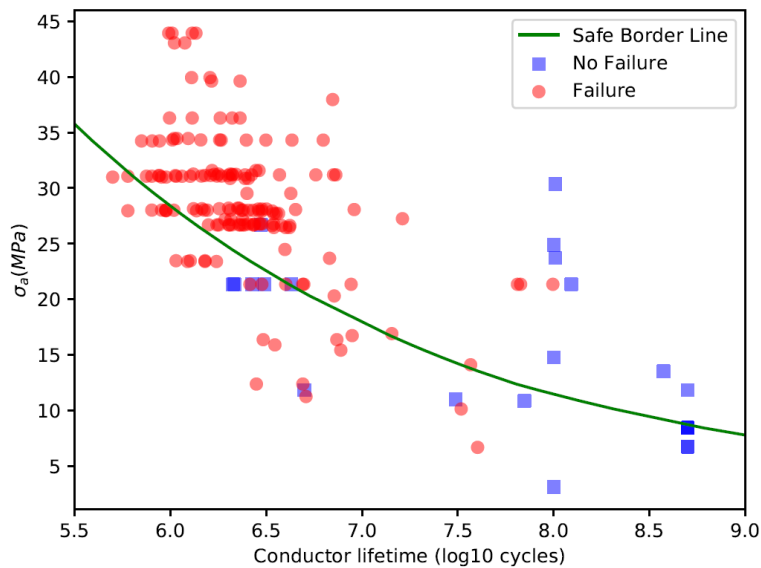
Figure 4: S-N plot of all experimental data gathered in the literature, with the SBL

In order to be conservative, all non-censored points (*i.e.* failures) should be located above the SBL. It would mean that the corresponding stress exceeded the recommended limit, hence the risk of failure begins to rise. However, this comparison reveals that even though most points are indeed located above it, some of them happen to be below the safe limit. This revealing observation highlights the fact the SBL tool may not be sufficient to ensure the mechanical strength of conductors for any condition reachable in laboratories. This motivates the intention of proposing a newer approach to address this topic. To complete the last assertion, it must be stated that the Safe Border Line was initially established for ACSR only. Still, as it will be detailed in the next section, these false negatives do not concern AAAC exclusively.

4.2. SBL versus quantile regressions

The plots on figure 5 sum up the comparisons that can be made between the fatigue data, the SBL and both bound regressions at 2.5% and 97.5%. As described earlier, both regression models depend on the conductor type (especially through K_{norm}). Thus, 4 plots are proposed with a single type of conductor for each plot. The normalized vibration amplitude Yb/D is set on the y-axis so these curves get similar to regular S-N curves.

These four comparisons reveal that even though the Safe Border Line remains accurate for some conductors (figures 5b and 5d) it can return a significant amount of false negatives for other types (figures 5a and 5c). This happens when non censored points (i.e. strand failures) are located below the SBL. This choice of plots also shows that this observation can be true for both AAAC and ACSR conductors. This means that in some cases, the SBL is not conservative enough to be applied for every power line design that there is.
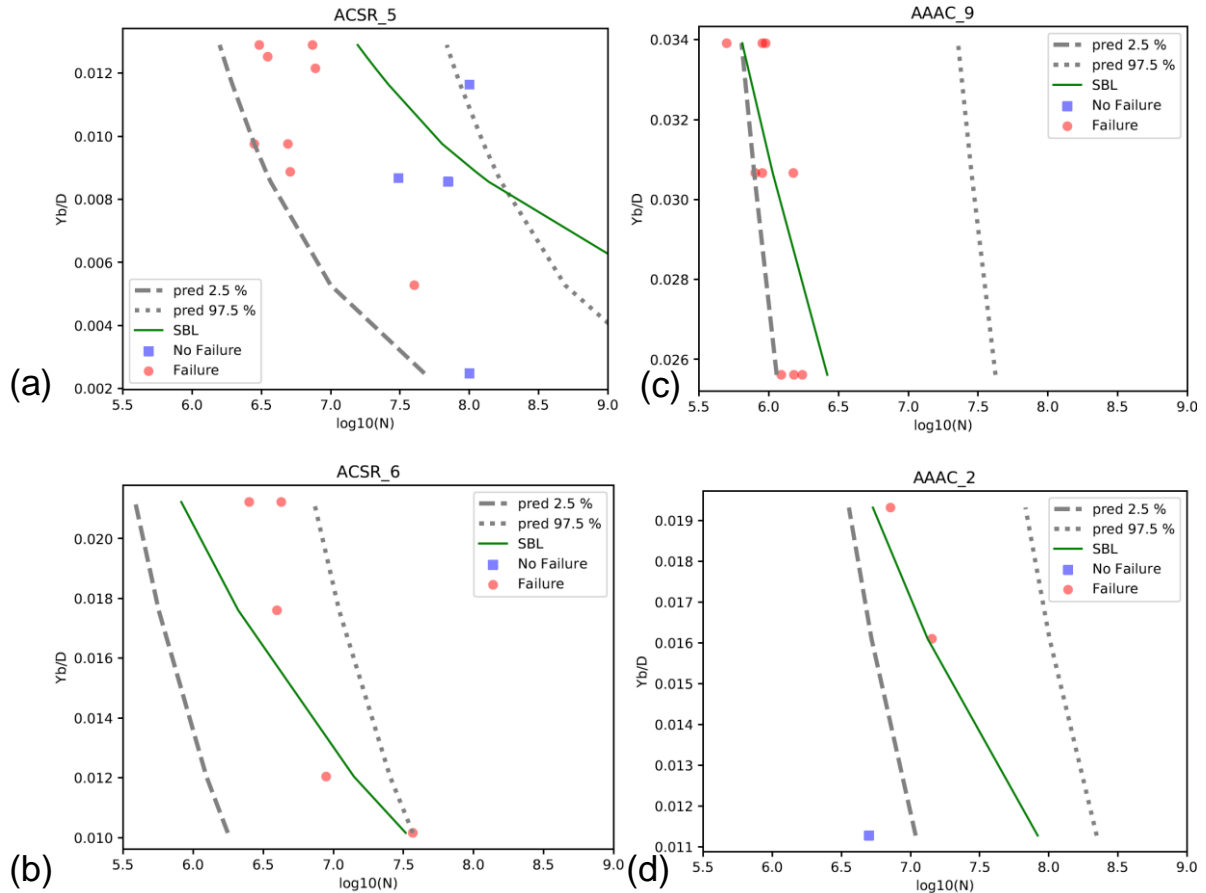
Figure 5: several Yb/D vs log(N) plots comparing experimental data, 2.5% and 97.5% quantile regressions and the Safe Border Line for 4 distinct types of conductor

On the other hand, the plot of the 2.5% quantile regressions shows that this model provides by definition a much stronger and reliable safe zone for predicting the occurrence of failure or not. It also remains very easy to use and directly available for anyone desiring to conduct such fatigue tests or even for future applications on the grid. On that matter, the 97.5 quantile regression may also be useful as it can offer the operator an estimate of the maximum lifetime for a test before even starting it, or for a line when it is being installed.

To deepen this comparison, figure 6 offers another point of view about how the 2.5% quantile regression vs the SBL behave. This figure plots every datapoint as a comparison between the actual experimental lifetime observed in laboratory versus the predicted lifetime. These theoretical durations can be obtained through both the SBL and the statistical models when they are used as predictive tools (for instance using the equation (9). If a point is located on the median y=x dotted line, it means that the prediction perfectly matches the test. If the point is below it, the prediction is conservative, and if it is above it, the

prediction is non conservative. Hence, this plots shows that the SBL is non conservative for several points, while the 2.5% quantile regression remains accurate or conservative at all times.
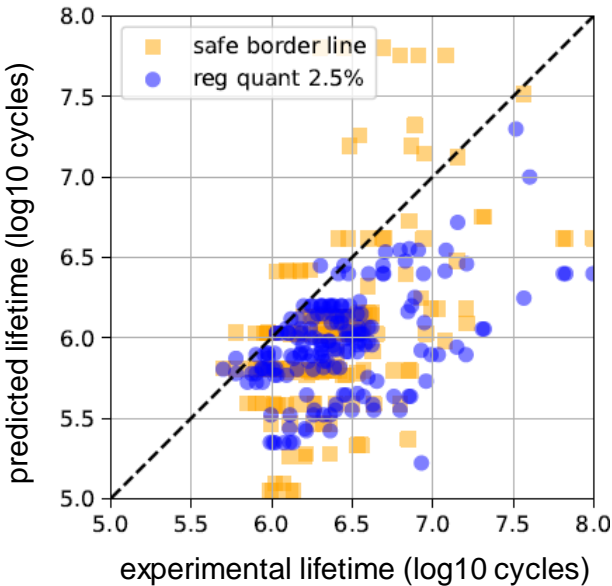
Figure 6: predicted lifetime versus experimental lifetime for the 2.5% quantile regression and the SBL

4.3. Discussion and perspectives

The proposed model described in the previous section gives promising results when a first set of conductor's fatigue tests is considered. However, these may be discussed according to their scope of application and future steps.

It can first be mentioned that most of these tests were conducted with rather severe loadings (with high RTS and Yb) in order to maximize the failure risk and being able to get as much information as possible from these expensive tests. One must keep in mind that most conductors endure less severe loadings throughout their lives. This may lead to possible errors when this model is used for more realistic boundary conditions that differ from the ones used to train this model. Still, as mentioned earlier, linear regressions such as the quantile one has a lower risk of "over-fitting", meaning it is rather resilient when extrapolated. More generally, new tests with more realistic loadings would be an interesting next step in order to check and test the model ability to predict all kinds of tests. These new tests may be with less severe loadings as well as similar ones to confirm the relevance of this approach. More work could also be achieved regarding the features themselves. Through better physical understanding of the mechanisms involved in the ageing mechanisms, other features may be considered, in addition or in replacement of those already described for this model.

Finally, it must be stated that in order to conduct a comprehensive study on such a complex topic, this fully statistical approach would have to be completed with additional physical modelling. As it is likely impossible to gather thousands of experimental data in the next years for various reasons, this lack of data could be compensated by developing physical models that could be chained with a statistical modelling layer. This would add more physical knowledge into the problem without relying only on experimental data

5 CONCLUSION

This paper presented a statistical approach based on experimental data on conductor's fatigue gathered from the literature. The following points were addressed:

- A table gathering more than 200 experimental tests on various conductors has been established, in order to help any TSO member willing to work on this topic. This dataset is directly suitable with statistical algorithms and regressions. It is displayed in the appendix and is available for anyone wishing to use it, whether it is for statistical analysis or other applications.

- The gathered tests were plotted versus the Safe Border Line, usually used to design and predict the occurrence of conductor's failure. It revealed that for these tests, the SBL was not conservative enough: some points located inside the safe zone still displayed failures.

- After defining the quantile regression algorithm, this model has been applied on the previous dataset, associated with four features. These explanatory variables are believed to be the most influent parameters on the behaviour of the conductor. It depends on the system geometry, materials and the boundary conditions. The corresponding coefficient were also given so anyone could use it at will.

- An alternate safe limit has been proposed with the 2.5% quantile regression. Compared with the SBL, this regression offered a promising design tool to ensure that any point within its safe zone would not undergo failure.

The purpose of this paper is to offer a simple and ready-to-use safe limit of overhead conductors enduring Aeolian vibrations, with proper description and justification. This approach can be applied for any type of conductor, but will offer the best results for ACSR and AAAC. This tool may be helpful for anyone working on this specific field, and can be more and more accurate as more experimental data are added into the training dataset.

6 BIBLIOGRAPHY

[1] W. G. Fricke and C. B. Rawlins, "Importance of Fretting in Vibration Failures of Stranded Conductors," *IEEE Trans. Power Appar. Syst.*, vol. 87, no. 6, pp. 1381–1384, 1968.

[2] G. Chen, X. Wang, J. Wang, J. Liu, T. Zhang, and W. Tang, "Damage investigation of the aged aluminium cable steel reinforced (ACSR) conductors in a high-voltage transmission line," *Eng. Fail.*

[3] R. B. Kalombo, J. A. Araújo, J. L. A. Ferreira, C. R. M. da Silva, R. Alencar, and A. R. Capra, "Assessment of the fatigue failure of an All Aluminium Alloy Cable (AAAC) for a 230 kV transmission line in the Center-West of Brazil," *Eng. Fail. Anal.*, vol. 61, no. August 2012, pp. 77–87, 2016.

[4] A. A. Fadel, D. Rosa, L. B. Murça, J. L. A. Fereira, and J. A. Araújo, "Effect of high mean tensile stress on the fretting fatigue life of an Ibis steel reinforced aluminium conductor," *Int. J. Fatigue*, vol. 42, pp. 24–34, 2012.

[5] C. R. F. Azevedo, A. M. D. Henriques, A. R. Pulino Filho, J. L. A. Ferreira, and J. A. Araújo, "Fretting fatigue in overhead conductors: Rig design and failure analysis of a Grosbeak aluminium cable steel reinforced conductor," *Eng. Fail. Anal.*, vol. 16, no. 1, pp. 136–151, 2009.

[6] G. E. Braga, R. Nakamura, and A. Furtado, "Aeolian vibration of Overhead Transmission Line Cables : Endurance Limits," *IEEE Transm. Distrib. Conf. Lat. Am.*, 2004.

[7] J. C. Poffenberger and R. L. Swart, "Differential Displacement and Dynamic Conductor Strain," *IEEE Trans. Power Appar. Syst.*, vol. 84, no. 4, pp. 281–289, 1965.

[8] Transmission Line Reference Book, Wind Induced Conductor Motion, EPRI – Electric Power Research Institue

[9] M. Miner, "Cumulative damage in fatigue," *J. Appl. Mech.*, no. 12, pp. 159–164, 1945.

[10] CIGRE WG 04 SC 22 – 02 Recommandations for the evaluation of the lifetime of transmission line conductors. Electra 63. March 1979

7 APPENDIX: EXPERIMENTAL DATA TABLE

conductor type	H (kN)	static angle (°)	Yb (mm)	number of cycles
ACSR	35.0	5.0	1.0	7026296
ACSR	35.0	5.0	0.8	102063666
ACSR	35.0	5.0	0.718	16249449
ACSR	35.0	5.0	0.656	100003108
ACSR	35.0	5.0	0.625	101966476
AAAC	36.6	5.0	0.3	500000000
AAAC	36.6	7.0	0.35	5000000
AAAC	36.6	6.5	0.35	500000000
AAAC	36.6	6.0	0.3	32900000
AAAC	36.6	7.0	0.5	14300000
AAAC	36.6	6.0	0.2	500000000
AAAC	36.6	7.0	0.6	7160000
AAAC	36.6	6.5	0.4	374000000
AAAC	36.6	6.5	0.2	500000000
AAAC	36.6	6.5	0.25	500000000
AAAC	36.6	6.5	0.7	6770000
AAAC	36.6	6.5	0.25	500000000
AAAC	36.6	6.5	0.25	500000000
AAAC	36.6	6.5	0.25	500000000
ACSR	45.0	6.0	0.6	99000000
ACSR	45.0	6.0	0.6	123510000
ACSR	45.0	6.0	0.6	67200000
ACSR	45.0	6.0	0.6	64700000
ACSR	45.0	6.0	0.6	2600000
ACSR	45.0	6.0	0.6	8770000
ACSR	45.0	6.0	0.6	3000000
ACSR	45.0	6.0	0.6	2120000
ACSR	45.0	6.0	0.6	2160000
ACSR	45.0	6.0	0.6	4000000
ACSR	45.0	6.0	0.6	4270000
ACSR	45.0	6.0	0.6	3100000
ACSR	45.0	6.0	0.6	2660000
ACSR	45.0	6.0	0.6	4900000
ACSR	45.0	6.0	0.6	4970000
ACSR	45.0	6.0	0.75	2090000
ACSR	45.0	6.0	0.75	2320000
ACSR	45.0	6.0	0.75	2030000
ACSR	45.0	6.0	0.75	2280000
ACSR	45.0	6.0	0.75	2970000
ACSR	45.0	6.0	0.75	1750000
ACSR	45.0	6.0	0.75	2020000
ACSR	45.0	6.0	0.75	2700000

conductor type	H (kN)	static angle (°)	Yb (mm)	number of cycles
ACSR	45.0	6.0	0.75	1580000
conductor type	H (kN)	static angle (°)	Yb (mm)	number of cycles
ACSR	45.0	6.0	0.75	1790000
ACSR	45.0	6.0	0.75	2440000
ACSR	45.0	6.0	0.75	2380000
ACSR	45.0	6.0	0.75	2730000
ACSR	23.0	10.0	0.813	16100000
ACSR	23.0	10.0	0.813	10840000
ACSR	23.0	10.0	0.813	24840000
ACSR	23.0	10.0	0.813	9760000
ACSR	23.0	10.0	0.789	8480000
ACSR	23.0	10.0	0.742	18620000
ACSR	23.0	10.0	0.695	102230000
ACSR	38.5	10.0	0.452	3050000
ACSR	38.5	10.0	0.452	7390000
ACSR	38.5	10.0	0.439	3510000
ACSR	38.5	10.0	0.426	7750000
ACSR	38.5	10.0	0.304	30760000
ACSR	38.5	10.0	0.3	70210000
ACSR	38.5	10.0	0.408	100000000
ACSR	54.0	10.0	0.744	4250000
ACSR	54.0	10.0	0.744	2510000
ACSR	54.0	10.0	0.617	3960000
ACSR	54.0	10.0	0.422	8880000
ACSR	54.0	10.0	0.356	36860000
ACSR	23.0	10.0	0.394	12110000
ACSR	23.0	10.0	0.394	8150000
ACSR	23.0	10.0	0.394	6260000
ACSR	38.5	10.0	0.342	2010000
ACSR	38.5	10.0	0.342	4910000
ACSR	38.5	10.0	0.342	2810000
ACSR	38.5	10.0	0.311	5100000
ACSR	38.5	10.0	0.185	40080000
ACSR	38.5	10.0	0.087	100000000
ACSR	23.0	10.0	0.84	4180000
ACSR	23.0	10.0	0.84	4000000
ACSR	23.0	10.0	0.84	3464000
ACSR	23.0	10.0	0.88	3670000
ACSR	23.0	10.0	0.88	3565000
ACSR	23.0	10.0	0.88	3464000
ACSR	23.0	10.0	0.98	2550000
ACSR	23.0	10.0	0.98	2450000
ACSR	23.0	10.0	0.98	2050000
ACSR	28.0	10.0	0.8	3460000
ACSR	28.0	10.0	0.8	3000000
ACSR	28.0	10.0	0.8	2900000

conductor type	H (kN)	static angle (°)	Yb (mm)	number of cycles
ACSR	28.0	10.0	0.84	3170000
ACSR	28.0	10.0	0.84	3000000
ACSR	28.0	10.0	0.84	2880000
ACSR	28.0	10.0	0.93	2000000
ACSR	28.0	10.0	0.93	1620000
ACSR	28.0	10.0	0.93	1515000
AAAC	22.0	10.0	0.71	1230000
AAAC	22.0	10.0	0.71	1515000
AAAC	22.0	10.0	0.71	1740000
AAAC	22.0	10.0	0.85	800000
AAAC	22.0	10.0	0.85	900000
AAAC	22.0	10.0	0.85	1500000
AAAC	22.0	10.0	0.94	500000
AAAC	22.0	10.0	0.94	900000
AAAC	22.0	10.0	0.94	950000
AAAC	26.0	10.0	0.68	1516000
AAAC	26.0	10.0	0.68	1270000
AAAC	26.0	10.0	0.68	1070000
AAAC	26.0	10.0	0.81	1370000
AAAC	26.0	10.0	0.81	950000
AAAC	26.0	10.0	0.81	600000
AAAC	26.0	10.0	0.9	800000
AAAC	26.0	10.0	0.9	750000
AAAC	26.0	10.0	0.9	600000
AAC	15.86	10.0	0.87	2550000
AAC	15.86	10.0	0.87	2750000
AAC	15.86	10.0	0.87	2950000
AAC	15.86	10.0	0.91	2350000
AAC	15.86	10.0	0.91	2550000
AAC	15.86	10.0	0.91	2700000
AAC	15.86	10.0	1.01	1450000
AAC	15.86	10.0	1.01	1750000
AAC	15.86	10.0	1.01	1850000
AAC	18.68	10.0	0.84	2380000
AAC	18.68	10.0	0.84	2070000
AAC	18.68	10.0	0.84	1930000
AAC	18.68	10.0	0.87	1800000
AAC	18.68	10.0	0.87	1460000
AAC	18.68	10.0	0.87	1320000
AAC	18.68	10.0	0.96	1270000
AAC	18.68	10.0	0.96	1150000
AAC	18.68	10.0	0.96	1070000
AAAC	20.54	10.0	0.82	4200000
AAAC	20.54	10.0	0.82	3800000
AAAC	20.54	10.0	0.82	3400000

conductor type	H (kN)	static angle (°)	Yb (mm)	number of cycles
AAAC	20.54	10.0	0.86	3400000
AAAC	20.54	10.0	0.86	3000000
AAAC	20.54	10.0	0.86	2900000
AAAC	20.54	10.0	0.96	2650000
AAAC	20.54	10.0	0.96	2450000
AAAC	20.54	10.0	0.96	2100000
ACSR	14.5	10.0	0.9	4500000
ACSR	14.5	10.0	0.9	9100000
ACSR	14.5	10.0	1.0	3710000
ACSR	14.5	10.0	1.0	7300000
ACSR	14.5	10.0	1.0	5740000
ACSR	14.5	10.0	1.0	7100000
ACSR	14.5	10.0	1.1	2490000
ACSR	14.5	10.0	1.1	4310000
ACSR	14.5	10.0	1.1	3150000
ACSR	14.5	10.0	1.1	1840000
ACSR	14.5	10.0	1.1	6270000
ACSR	14.5	10.0	1.27	1640000
ACSR	14.5	10.0	1.27	2310000
ACSR	14.5	10.0	1.38	1190000
ACSR	14.5	10.0	1.38	1050000
ACSR	22.75	10.0	0.87	2790000
ACSR	22.75	10.0	0.87	2900000
ACSR	22.75	10.0	0.87	1650000
ACSR	22.75	10.0	1.0	990000
ACSR	22.75	10.0	1.0	2100000
ACSR	22.75	10.0	1.0	2310000
ACSR	22.75	10.0	1.0	1820000
ACSR	22.75	10.0	1.0	1300000
ACSR	22.75	10.0	1.1	1610000
ACSR	22.75	10.0	1.1	1290000
ACSR	22.75	10.0	1.21	980000
ACSR	22.75	10.0	1.21	1020000
ACSR	22.75	10.0	1.21	1360000
ACSR	22.75	10.0	1.21	1300000
AAAC	25.84	10.0	0.92	2244600
AAAC	25.84	10.0	0.92	2283300
AAAC	25.84	10.0	0.92	2012400
AAAC	25.84	10.0	1.02	2051100
AAAC	25.84	10.0	1.02	1780200
AAAC	25.84	10.0	1.02	1316736
AAAC	25.84	10.0	1.12	1807488
AAAC	25.84	10.0	1.12	1440504
AAAC	25.84	10.0	1.12	1024668
AAAC	30.4	10.0	0.87	2052918

conductor type	H (kN)	static angle (°)	Yb (mm)	number of cycles
AAAC	30.4	10.0	0.87	1560384
conductor type	H (kN)	static angle (°)	Yb (mm)	number of cycles
AAAC	30.4	10.0	0.87	2395008
AAAC	30.4	10.0	0.97	2201400
AAAC	30.4	10.0	0.97	1695096
AAAC	30.4	10.0	0.97	2110374
AAAC	30.4	10.0	1.07	1238724
AAAC	30.4	10.0	1.07	1044900
AAAC	30.4	10.0	1.07	1083600
AAAC	38.0	10.0	0.81	945342
AAAC	38.0	10.0	0.81	945342
AAAC	38.0	10.0	0.81	1043136
AAAC	38.0	10.0	0.9	869184
AAAC	38.0	10.0	0.9	1060704
AAAC	38.0	10.0	0.9	877824
AAAC	38.0	10.0	0.99	877824
AAAC	38.0	10.0	0.99	803700
AAAC	38.0	10.0	0.99	707256
AAAC	26.44	10.0	0.8	2000000
AAAC	26.44	10.0	0.8	1900000
AAAC	26.44	10.0	0.8	1700000
AAAC	26.44	10.0	0.89	1500000
AAAC	26.44	10.0	0.89	1200000
AAAC	26.44	10.0	0.89	1080000
AAAC	26.44	10.0	0.89	1000000
AAAC	26.44	10.0	0.98	1800000
AAAC	26.44	10.0	0.98	1480000
AAAC	26.44	10.0	0.98	1080000
AAAC	26.44	10.0	0.98	590000
AAAC	30.29	10.0	0.86	4000000
AAAC	30.29	10.0	0.86	3000000
AAAC	30.29	10.0	0.96	2400000
AAAC	30.29	10.0	0.96	1300000
AAAC	30.29	10.0	1.0	1700000
AAAC	30.29	10.0	1.06	1500000
AAAC	30.29	10.0	1.06	1510000